and M. Baldwin, J. Appl. Phys. 34, 1137 (1963).
[17]R. Heritage, A. Young, and I. Bolt, Brit. J. Appl. Phys. 14, 439 (1963).
[18]R. Prosen, B. Gran, J. Kivel, C. Searle, and A. Morrish, J. Appl. Phys. 34, 1147 (1963).
[19]C. Kennedy, Master's thesis (Ohio State University, Columbus, 1969).
[20]G. Bailey (unpublished).
[21]R. Spain, Appl. Phys. Letters 6, 8 (1965).
[22]G. Weiss and D. Smith, J. Appl. Phys. 33, 1166 (1962).
[23]Z. Frait and M. Ondris, Czech. J. Phys. B 11, 885 (1961).
[24]D. Bagguley, Proc. Phys. Soc. (London) B67, 549 (1954).
[25]T. Phillips, Proc. Roy. Soc. (London) A292, 224 (1966).

PHYSICAL REVIEW B VOLUME 5, NUMBER 11 1 JUNE 1972

Temperature Dependence of Phonon Raman Scattering in $FeBO_3$, $InBO_3$, and VBO_3: Evidence for a Magnetic Contribution to the Intensities

I. W. Shepherd*
Central Research Department,† E. I. du Pont de Nemours and Company, Experimental Station, Wilmington, Delaware 19898
(Received 25 August 1971)

The complete Raman spectra comprised of $4E_g$ and $1A_{1g}$ modes have been observed in four materials of calcite structure (point group D_{3d}) from 15 to 400 °K: ferromagnetic VBO_3 (T_c = 32.5 °K), antiferromagnetic $FeBO_2$ (T_c = 350 °K) and $Fe_{0.9}Ga_{0.1}BO_3$ (T_c = 272 °K), and nonmagnetic $InBO_3$. The energies of the modes are similar in all samples, with approximate values of 930 cm^{-1} (A_{1g}) and 1210, 650, 400, and 270 cm^{-1} (E_g), and show no significant shift over the temperature range studied. Observed intensity variations with temperature of three lines in $InBO_3$ relative to the A_{1g} symmetric mode are consistent with changes in phonon population with temperature. Large variatiations in intensity of lines relative to the A_{1g} modes were observed in the region of T_c which were qualitatively similar in all three magnetic materials. At high temperatures ($T > 6T_c$) in VBO_3 the intensity changes with temperature were consistent with phonon population changes. The intensity changes in the magnetic crystals are attributed to a phonon-magnon interaction arising from an exchange coupling which depends on ion position. No scattering from magnons was observed in the borates, but the temperature dependence of a line in the spectrum of the structurally related (point group D_{3d}) transparent antiferromagnet FeF_3 was characteristic of magnon scattering.

I. INTRODUCTION

Recent scattering experiments on magnetic materials have demonstrated the influence of magnetic order on the phonon Raman spectrum.[1,2] The material studied in Ref. 2 was $FeBO_3$ which is a transparent canted antiferromagnet having calcite structure (point group D_{3d})[3]; the materials studied in Ref. 1 were the semiconducting chalcogenide spinels, $CdCr_2Se_4$ (T_c = 130 °K) and $CdCr_2S_4$ (T_c = 85 °K), both of which are ferromagnetic and highly absorbing in the visible region of the spectrum.[4-7] Despite their very different physical properties, the Raman spectra in all these materials show similar significant intensity variations with temperature in the region of the Curie points. These intensity changes may possibly be attributed to an interaction between spin system and phonons.[8] Infrared absorption measurements in CoF_2, which also showed temperature-dependent intensities, were explained by an interaction between magnetic excitations and phonons[9]; other related papers[10,11] include the electron-hole interaction in discussions of optical absorption in magnetic semiconductors.

The present work extends the study[2] of $FeBO_3$ to two other materials, VBO_3 and $InBO_3$, which have the same structure as $FeBO_3$ while differing markedly in their magnetic properties. The small saturation magnetization of 2.07 emu/g in $FeBO_3$ (T_c = 350 °K) results from the canting of the two magnetic sublattices.[3] The much larger magnetization of 83.5 emu/g observed in VBO_3 (T_c = 32.5 °K) is equivalent to 1.64 μ_B per V^{3+} ion.[12] Although this is smaller than the expected value of 2 μ_B it does indicate that VBO_3 is a true ferromagnet. $InBO_3$ is, of course, nonmagnetic. There are two experimental advantages to dealing with these borate compounds. First, they are highly transparent to the exciting laser radiation which leads to excellent signal-to-noise ratios. Second, the calcite structure has a simple Raman spectrum of five allowed modes, one of symmetry A_{1g} and four E_g. All these are observed and easily identified in the crystals studied here. A comparison of the Raman spectra as a function of temperature in $FeBO_3$ and VBO_3 should cast some light on the

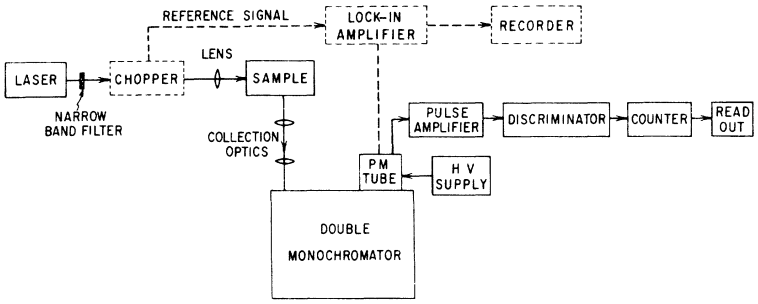

FIG. 1. Schematic diagram of Raman-scattering equipment.

effect of the type of magnetic ordering on the coupling between phonons and magnetic spins. For comparison, $InBO_3$ is expected to show no magnetic effects, the only temperature dependence arising from phonon population effects.

II. EXPERIMENTAL DETAIL

Single crystals of $FeBO_3$ with planar growth surfaces approximately 1 mm long were grown under pressure by Dr. T. A. Bither from starting material in which Fe was the only cation. The Curie temperature[13] was 350 °K. Samples with 10-at.% Ga doping were grown by Dr. L. H. Brixner using a flux technique. These $Fe_{0.9}Ga_{0.1}BO_3$ samples were platelets of area up to 1 cm^2 and thickness 0.2 mm, and the Curie temperature was 270 °K. Both these samples were green with an absorption minimum at 5200 Å. Single crystals of VBO_3 were grown under pressure.[12] The crystals were deep red, but as they were small (< 0.3-mm linear dimension), a compressed pellet was used for the Raman experiments. The $InBO_3$ crystals were grown by Dr. R. D. Shannon and were colorless transparent platelets of thickness 0.2 mm and area up to 1 cm^2. All the material growth was carried out in this laboratory.

A schematic diagram of the Raman spectrometer is shown in Fig. 1. The mode of operation for $FeBO_3$ and $InBO_3$ was to excite the Raman spectrum using the 5145-Å line of an argon laser and to detect using a S-20 photomultiplier and photon counting. Because of the high absorption of VBO_3 in the green, a Nd^{+++} yttrium aluminum garnet (YAG) laser at 1.06 μ was used as source, and an S-1 photomultiplier for detection. The relatively high dark current of a tube with S-1 response made an ac technique most effective with the reference signal obtained from a mechanical chopper in the laser beam. The laser beam was focused onto the sample which was held in a helium-exchange-gas cryostat. The temperature could be varied from 4.2 to 400 °K with control of ± 1 °K. With laser power of approximately 500 mW focused to a spot of diameter 0.3 mm, the largest sample heating observed, which occurred for the VBO_3 pellet, was 20 °K above ambient. This temperature differential was measured by comparing the relative sizes of Stokes and anti-Stokes signals. The problem of estimating the sample temperature is most severe for VBO_3 because of the low signal-to-noise ratio and the fast changing photomultiplier response. The response of the S-1 tube, measured using a tungsten source and corrected for the small change in output, decreased by a factor of 1.75 between the anti-Stokes and Stokes components of the 260-cm^1 line. This factor was taken into account in obtaining the ratio used to calculate the temperature. The best accuracy was obtained in the region of $T = 150$ °K, where the VBO_3 anti-Stokes line at 260 cm^{-1} was still clearly visible yet the temperature was low enough to make the ratio a sensitive function of temperature. The estimated error in sample temperature was ± 6 °K. In the helium-temperature region where the anti-Stokes signals were not visible, the differential was assumed to be the same as that at higher temperatures for the same sample and incident power density. The scattered light was collected at 90° to the laser beam and passed through a double monochromator to the detecting photomultiplier.

III. RESULTS

The Raman spectra were obtained over the following temperature ranges: $FeBO_3$ and $Fe_{0.9}Ga_{0.1}BO_3$, 20 – 380 °K, $InBO_2$, 79 – 330 °K, and VBO_3, 15 – 310 °K, where all temperatures were corrected for laser heating effects. Sample spectra are shown in Fig. 2. The relatively poor signal-to-noise ratios in the VBO_3 spectrum, caused by the low quantum efficiency of the S-1 photomultiplier, are particularly noticeable at the higher energies where the extreme end of the photomultiplier response is being approached. The spectrum of $Fe_{0.9}Ga_{0.1}BO_3$, which is not shown, is indistinguishable from that of $FeBO_3$ within the experimental error of ± 1 cm^{-1}. This is not surprising as the phonon modes do not involve motion of the cation. Except for $FeBO_3$ which has an extra line at 535 cm^{-1}, five lines are visible in each trace representing the complete Raman spectra.

In the calcite structure only two phonon symmetries are allowed, A_{1g} and E_g. The easiest way of

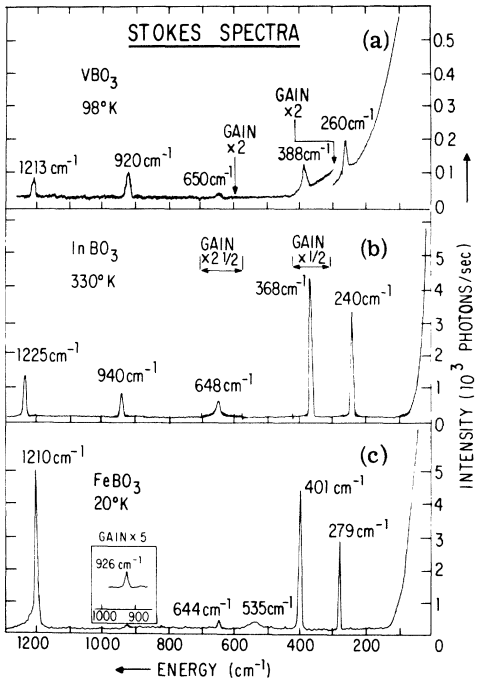

FIG. 2. Stokes Raman spectra of the Fe, V, and In borates. (c) has been published previously (Ref. 2).

differentiating between these is to measure the $\{ZZ\}$ component of the Raman tensor which is zero for E_g and finite for A_{1g}.[14] This procedure was accomplished in the cases of $FeBO_3$ and $InBO_3$, where single crystals were available, by using appropriate scattering geometry and polarizations. The particular molecular assignments were made in conjunction with infrared data.[15] In the case of VBO_3, where single crystals were not available, the assignments were made by comparing the spectrum with the spectra of the other two compounds.

TABLE I. Positions of phonon Raman lines in three borates at various temperatures. The numbers in parentheses indicate linewidths measured with 4-cm^{-1} slits. The slits had to be opened to 10 cm^{-1} to obtain satisfactory traces of the weaker lines (see Fig. 2) and the observed widths were instrumentally limited. No values have been given in these cases.

Material	Temperature (°K)	Line positions and widths (cm^{-1})				
$InBO_3$	79	241(4)	370(6)	648	940(8)	1226(6)
	330	240(6)	368(7)	648	938(9)	1225(7)
$FeBO_3$ and $Fe_{0.9}Ga_{0.1}BO_3$	20	279(4)	401(5)	644	926	1210(5)
	85	279(4)	401(5)	644	926	1210(5)
	380	278(5)	397(7)	641	921	1210(7)
VBO_3	15	261(6)	389(7)	···	922	1214
	98	260(8)	388(8)	650	920	1213
	310	260(9)	387(8)	650	920	1213

Reference to Fig. 2 shows that the comparison is unambiguous. The lines in the regions 1200 cm^{-1} (E_g), 900 cm^{-1} (A_{1g}), and 600 cm^{-1} (E_g) arise, respectively, from the asymmetric breathing mode (ν_3), the symmetric mode (ν_1), and the in-plane bending mode (ν_4) of the BO_3^{3-} molecule; the lines near 400 cm^{-1} and between 200 and 300 cm^{-1} have symmetry E_g and arise from lattice modes. All these lines except the symmetric modes are infrared active.[15] Details of the line positions and widths at different temperatures are given in Table I, and clearly there are no large shifts or broadenings. Each material will now be discussed separately for the purpose of presenting intensity variations as a function of temperature.

A. $InBO_3$

The intensity ratios of three of the lines with the 938-cm^{-1} line are plotted against temperature in Fig. 3. (The measurement of the small line at 648 cm^{-1} was too inaccurate for inclusion.) The lines represent the theoretical dependence calculated from the phonon-population factor $(n+1)$ and normalized to the experimental point at lowest temperature. The expression for the population factor is

$$n+1=\frac{1}{e^x-1}+1 \quad , \tag{1}$$

where $x=\hbar\omega_0/kT$ and ω_0 is the phonon Raman shift. The agreement between theory and experiment indicates that phonon population changes cause the only temperature effect on the Raman intensities. These nonmagnetic data provide a comparison for the equivalent plots of the magnetic borates (Figs. 5 and 6).

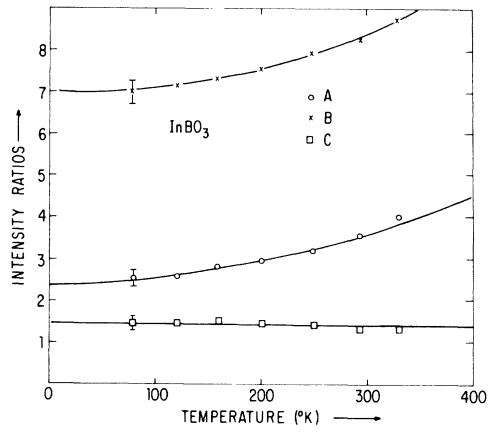

FIG. 3. Ratios of intensities of the (a) 240-, (b) 368-, and (c) 1225-cm^{-1} lines to the 938-cm^{-1} line plotted as a function of temperature for $InBO_3$. The curves represent the theoretical predictions based on the temperature dependence of phonon populations.

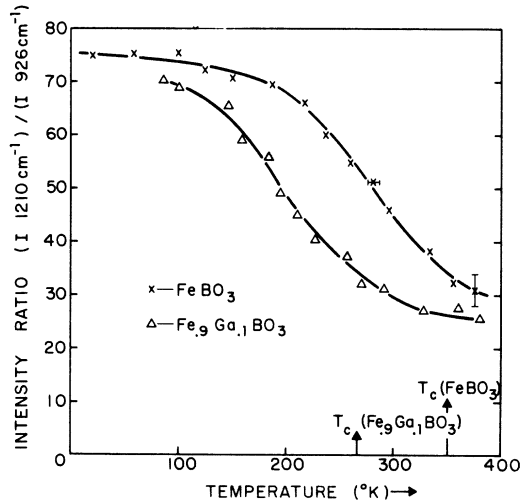

FIG. 4. The intensity ratio of the 1210 cm^{-1} to the 926-cm^{-1} Raman line plotted as a function of temperature. The crosses refer to pure $FeBO_3$ and the triangles to $Fe_{0.9}Ga_{0.1}BO_3$. The two curves show a similar decrease with increasing temperature, but are shifted along the temperature axis by the difference in the Curie temperature T_c. This figure has been published previously (Ref. 2).

B. $FeBO_3$ and $Fe_{0.9}Ga_{0.1}BO_3$

The intensity ratio of the 1210-cm^{-1} line with the 926-cm^{-1} line is plotted in Fig. 4 both for pure $FeBO_3$ and for the gallium-doped material. Both curves are similar in shape and show that the 1210-cm^{-1} line decreases significantly as the temperature is raised. The effect of the phonon population on the temperature dependence of this ratio is expected to be small and to be comparable with that shown in curve C of Fig. 3. The temperature separation of the curves by the difference in their respective Curie temperatures demonstrates unambiguously that the intensity change is associated with the magnetic order. The intensity ratios of the 1210-, 644-, 401-, and 279-cm^{-1} lines to the 926-cm^{-1} line for pure $FeBO_3$, plotted in Fig. 5, decrease as the temperature rises through T_c. The effect of the phonon population would be to increase the ratios with increasing temperature for the 644-, 401-, and 279-cm^{-1} lines as indicated in Fig. 3. A correction for this effect would thus serve to accentuate the temperature variation shown.

All ratios have been plotted relative to the symmetric mode, and thus some discussion of the intensity variation of this mode is relevant. Within the limits of experimental error the A_{1g} intensity was found to be constant in all materials over the temperature ranges covered. However, it is extremely difficult to compare absolute intensities from one temperature run to another, and in the present experiment the error is estimated to be as much as 20% over the range studied. (Indeed, it is to overcome this problem that the results are presented in the form of ratios.) It is thus not possible to determine whether or not the A_{1g} mode follows a temperature dependence determined solely by phonon population effects, which would amount to an intensity increase of only 3% between 0 and 380 °K. There may be a dependence of the A_{1g} mode on magnetization which is smaller than the experimental error. However, on the evidence of the temperature dependence of the ratios, any magnetic effects must be smaller for this mode than for the E_g modes.

The line at 535 cm^{-1} observed at 20 °K (Fig. 2) does not fit in the pattern of the Raman spectra as observed in the other two compounds. It is already broader than the other five lines in $FeBO_3$ at 20 °K and was observed to broaden further as the temperature increased until it disappeared at 85 °K. The fact that it has a relatively large energy that does not detectably change with temperature and that it disappeared before the temperature reached $\frac{1}{4}T_c$ seems to preclude the assignment of this line to a magnon. Although the origin of this line is presently not understood, it should be mentioned that the temperature-dependent behavior

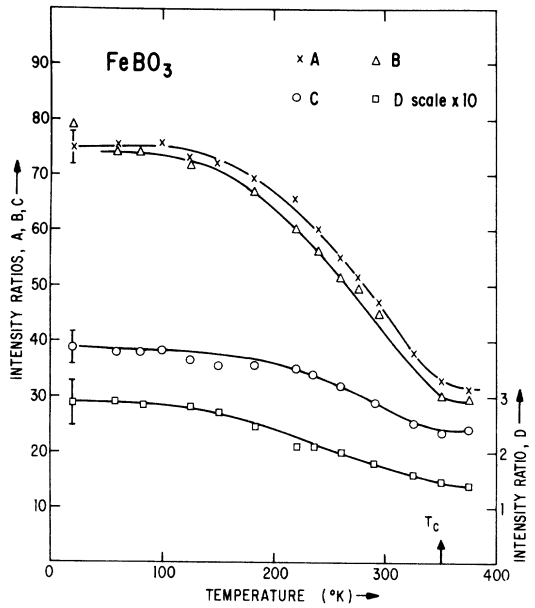

FIG. 5. Ratios of the intensities of the (a) 1210-, (d) 644-, (b) 401-, and (c) 279-cm^{-1} lines to the 926-cm^{-1} line plotted vs temperature for pure $FeBO_3$. The ordinate scale for the 644-cm^{-1} ratio is expanded × 10. All curves show a similar decrease as the temperature increases through the Curie temperature ($T_c = 350$ °K). No correction has been made for the $(n+1)$ temperature dependence. This figure has been published previously (Ref. 2).

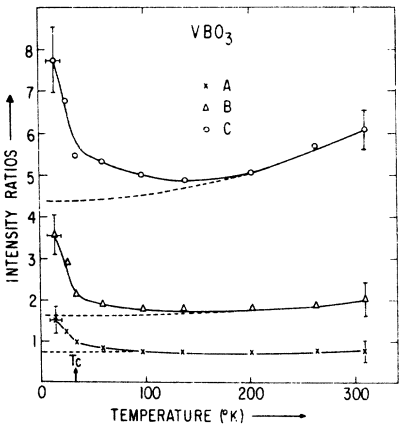

FIG. 6. Ratios of the intensities of the (a) 1213-, (b) 387-, and (c) 260-cm^{-1} lines to the 920-cm^{-1} line plotted vs temperatures for VBO_3. All curves show a decrease as the temperature increases through the Curie temperature ($T_c = 32.5\,°K$). The dashed lines represent the theoretical predictions based on the temperature dependence of the phonon populations.

is characteristic of a local impurity mode. In any event, this mode is assumed not to be part of the intrinsic phonon Raman spectrum of $FeBO_3$.

C. VBO_3

The intensity ratios of three of the lines with the 920-cm^{-1} line are plotted against temperature in Fig. 6. The line at 650 cm^{-1} has been omitted as it was too weak for accurate measurement. Because of the severe temperature-control problems arising from laser heating and the low value of $T_c = 32.5\,°K$, data were taken at only two points below T_c. Even when allowance is made for the inaccuracy of the temperature measurements in this region, it is clear that the ratios all decrease as the temperature increases through T_c. A compensating advantage of the low T_c is that the temperature range covered extends to almost 10 T_c which is well out of the region where magnetic effects are important. The ratios of the 260- and 387-cm^{-1} lines are seen to increase above 200 °K ($6T_c$) in a manner consistent with phonon population changes. The dashed lines represent the theoretical predictions based on Eq. (1) and normalized at the highest temperature 310 °K.

IV. DISCUSSION

The intensities of the complete phonon Raman spectrum in $InBO_3$ vary according to thermal population changes over the temperature range studied. Spectra of the magnetic materials, VBO_3 and $FeBO_3$, show large variations in intensity with temperature that are clearly connected with magnetic order. These data are not believed to result from magnon scattering[16] because no decrease in frequency was observed near T_c and because the positions of the lines correlate well with the phonon modes in nonmagnetic $InBO_3$ and in VBO_3 at high temperatures, where no magnetic influence is expected. It appears, then, that we are dealing with systems that demonstrate a magnetic effect on the phonon Raman spectrum. It can be assumed with reasonable accuracy that the magnetization in $FeBO_3$ follows the Brillouin function with spin equal to $\frac{5}{2}$, which results from the molecular field model of ordered magnetic solids.[17] Knowing that $T_c = 350\,°K$, the reduced magnetization can be calculated at the temperature of each experimentally determined Raman ratio (Fig. 5). The resulting plots of ratios $\frac{1210}{926}$ and $\frac{279}{926}$ against reduced magnetization are shown in Fig. 7. The dependence is approximately linear, and the gradient gives a measure of the strength of the magnetic effect. The same technique could be applied to VBO_3, where the spin value is 1, but because of the problems in temperature measurement only three points were taken below T_c and these are not sufficient for a meaningful plot. It is clear that in the case of VBO_3 the dependence is more complicated than linear because there is a clearly visible excess over the phonon contribution up to $T \sim 6T_c$ (Fig. 6). A similar dependence that extended well above T_c was observed[1] in $CdCr_2Se_4$ and agreed closely with the spin correlation function calculated from a two-spin cluster theory.[18] A possible theoretical explanation has been proposed by Baltensperger[8] who uses a bilinear spin Hamiltonian. Thus

$$H_M = \sum_{nm} S_m J_{mn} S_n \ , \qquad (2)$$

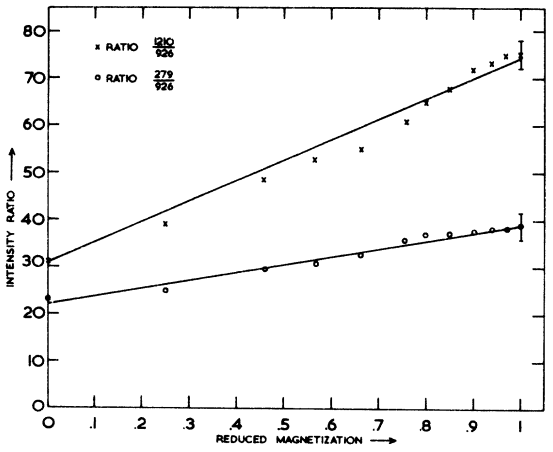

FIG. 7. Ratios of Raman intensities of 1210- and 279-cm^{-1} lines to the 976 cm^{-1} line in $FeBO_3$ plotted vs reduced magnetization. The values of reduced magnetization were calculated at the temperature of each experimentally determined ratio (Fig. 5) assuming a Brillouin dependence with spin $\frac{5}{2}$ and $T_c = 350\,°K$. The dependence of Raman intensity on magnetization is approximately linear.

where the exchange constant J_{mn} depends on the ion position R,

$$J_{mn}(R) = J_{mn}(R_0) + (\nabla J_{mn})_{R=R_0}\,\delta R, \tag{3}$$

and so produces a coupling between spin system and phonons.[19] A quantitative comparison between theory and experiment will, however, only be possible following detailed calculations for the various modes.

ACKNOWLEDGMENTS

The author wishes to acknowledge helpful discussions with Dr. H. S. Jarrett and Dr. C. W. Haas.

*Present address: Physics Department, University of Manchester, Manchester M13 9PL, England.

†Contribution No. 1848.

[1]E. F. Steigmeier and G. Harbeke, Phys. Kondensierten Materie 12, 1 (1970).

[2]I. W. Shepherd, J. Appl. Phys. 42, 1482 (1971).

[3]R. Wolfe, A. J. Kurtzig, and R. C. LeCraw, J. Appl. Phys. 41, 1218 (1970); A. J. Kurtzig, R. Wolfe, R. C. LeCraw, and J. W. Nielson, Appl. Phys. Letters 14, 350 (1969).

[4]P. K. Baltzer, H. W. Lehmann, and M. Robbins, Phys. Rev. Letters 11, 493 (1965); N. Menyuk, K. Dwight, R. J. Arratt, and A. Wold, J. Appl. Phys. 37, 1387 (1966).

[5]H. W. Lehmann and M. Robbins, J. Appl. Phys. 37, 1389 (1966).

[6]P. K. Baltzer, P. J. Wojtowicz, M. Robbins, and F. Lopatin, Phys. Rev. 151, 367 (1966).

[7]G. Herbeke and H. Pinch, Phys. Rev. Letters 17, 1090 (1966).

[8]W. Baltensperger, J. Appl. Phys. 41, 1052 (1970).

[9]S. J. Allen and H. J. Guggenheim, Phys. Rev. Letters 21, 1807 (1968).

[10]R. M. White, Phys. Rev. Letters 23, 858 (1969).

[11]T. Kambara and Y. Tanabe, J. Phys. Soc. Japan 28, 628 (1970).

[12]T. A. Bither, Carol G. Frederick, T. E. Gier, J. F. Weiher, and H. S. Young, Solid State Commun. 8, 109 (1970).

[13]All Curie-temperature measurements were performed in this laboratory by Carol G. Frederick.

[14]R. Loudon, Advan. Phys. 13, 423 (1964).

[15]K. Nakamoto, *Infrared Spectra of Inorganic and Coordination Compounds* (Wiley, New York, 1970), p. 96.

[16]It is not understood at present why magnon scattering is not observed in $FeBO_3$ whereas in the closely related material (Ref. 3) FeF_3, a line, which may well be due to a magnon, was observed to shift in energy from 183 to 154 cm^{-1} as the temperature increased towards T_c.

[17]See, for example, C. Kittel, *Introduction to Solid State Physics* (Wiley, New York, 1968), p. 458.

[18]E. Callen, Phys. Rev. Letters 20, 1045 (1968).

[19]The ion position dependence of the exchange interaction has also been used to calculate frequency changes of optical phonons caused by magnetic ordering. W. Baltensperger and J. S. Helman, Helv. Phys. Acta 41, 668 (1968).

PHYSICAL REVIEW B VOLUME 5, NUMBER 11 1 JUNE 1972

Corrections to Scaling Laws*

Franz J. Wegner†

Department of Physics, Brown University, Providence, Rhode Island 02912

(Received 14 January 1972)

The effects of higher-order contributions to the linearized renormalization group equations in critical phenomena are discussed. This analysis leads to three quite different results: (i) An exact scaling law for redefined fields is obtained. These redefined fields are normally analytic functions of the physical fields. Corrections to the standard power laws are derived from this scaling law. (ii) The theory explains why logarithmic terms can exist in the free energy. (iii) The case in which the energy scales like the dimensionality is analyzed to show that quite anomalous results may be obtained in this special situation.

I. INTRODUCTION

It has been shown by several authors[1-3] that a linearized form of the renormalization group equations leads to scaling laws for critical phenomena. In this paper we use the renormalization group equations to obtain corrections to the well-known[4] power laws for the singular part of the free energy and for the expectation values of different operators and susceptibilities.

The free energy of a magnetic system and of superfluid helium as a function of the symmetry breaking field h and $\tau \propto T - T_c$ is obtained as an expansion

$$F = g_0 + |g_E|^{2-\alpha} f^{\pm}\left(\frac{\beta h}{|g_E|^{\Delta}}\right) + \sum_i g_i |g_E|^{2-\alpha-\Delta i} f_i^{\pm}\left(\frac{\beta h}{|g_E|^{\Delta}}\right) + \ldots \tag{1.1}$$

in which the redefined fields g_0, g_E, and g_i are analytic functions of $\tau \propto T - T_c$ unless certain relations are fulfilled (see below). The function g_E vanishes for $\tau = 0$, $g_E = \tau + O(\tau^2)$. The first term g_0